Received December 18, 2018, accepted January 10, 2019, date of publication January 15, 2019, date of current version April 12, 2019.

*Digital Object Identifier 10.1109/ACCESS.2019.2892993*

# Energy-Aware Virtual Optical Network Embedding in Sliceable-Transponder-Enabled Elastic Optical Networks

**MIN ZHU[1], QING SUN[2], SHENGYU ZHANG[2], PAN GAO[2], BIN CHEN[2], AND JIAHUA GU[2]**

[1]National Mobile Communications Research Laboratory, Southeast University, Nanjing 210096, China
[2]School of Electronic Science and Engineering, Southeast University, Nanjing 210096, China

Corresponding author: Min Zhu (minzhu@seu.edu.cn)

This work was supported by the National Natural Science Foundation of China under Grant NSFC 61771134.

**ABSTRACT** Network virtualization has been widely considered to improve the resource efficiency of network infrastructure by allowing multiple virtual networks to coexist on a shared substrate network. With the exponential growth of Internet traffic, the network energy consumption incurs a considerable increase around the world. In this paper, we consider energy-aware virtual optical network embedding (EA-VONE) issue in flexible-grid elastic optical networks (EONs), while sliceable transponders (TPs) are assumed to be equipped in each node. First, an integer linear programming (ILP) model for the energy-minimized VONE is developed to optimally solve this problem. Due to the non-scalability of the ILP model, we then design two energy-saving policies for data centers (DCs) and TPs in the process of the node mapping and link mapping, respectively. Based on the two policies, two heuristic schemes are also developed: 1) DC-EA scheme, which only considers DC energy-saving in the node mapping procedure and 2) DC&TP-EA scheme, which simultaneously considers the energy-saving for both the DCs in the node mapping and TPs in the link mapping. Moreover, offline and online EA-VONE algorithms are developed. To investigate the benefits of the two energy-saving (i.e., DC-EA and DC&TP-EA) schemes, a benchmark scheme is also realized, which only maintains traffic-balancing (TB) policy without any energy-saving consideration. The simulation results indicate that our proposed DC&TP-EA scheme achieves the maximum power saving efficiency compared with the DC-EA and TB schemes. Also, in the DC-EA and DC&TP-EA schemes, the effect of DC energy saving is very remarkable when the traffic load is smaller. With the increase of traffic load, the DC energy saving may matter less, meanwhile, the TP energy-saving plays a more and more important role. Moreover, both the DC&TP-EA and DC-EA schemes maintain similar blocking performance as that of the TB scheme, which shows the superiority of our proposed schemes.

**INDEX TERMS** Energy efficiency, dynamic virtual optical network embedding, data center, sliceable transponder.

## I. INTRODUCTION

The recent booming of cloud-based applications has been stimulating the research and development on the on-demand provision of computing, storage and network resources over future optical networks connecting with geographically distributed data centers (DCs) [1]. Moreover, with the exponential growth of Internet traffic, the network and DC resource energy consumption incurs a considerable increase around the world. Estimates indicate that the annual energy bill paid by DC operators will exceed the cost of equipment [2]. As a result, building green energy-saving inter-DC substrate networks to reduce energy consumption has recently become the major concerns of internet service providers (ISPs).

Network virtualization is emerging as a promising solution to greatly enhance the flexibility and scalability of substrate optical network (SON). Meanwhile, the network virtualization can greatly improve the resource utilization and enhance the energy efficiency by allowing multiple virtual optical networks (VONs) to exist on a shared SON. Specifically,

The associate editor coordinating the review of this manuscript and approving it for publication was Sanaa Sharafeddine.

a VON can be constructed for each application, and multiple VONs share these resources in the same physical SON [3]. The process of the VON construction has been widely studied in the literature as VON embedding (VONE), which generally comprises the following two steps in turn: 1) *node mapping*, which is placing virtual nodes (VNs) onto *different* substrate nodes (SNs), and after that, 2) *link mapping*, which is provisioning virtual optical links (VOLs) onto physical lightpaths with so-called routing and spectrum allocation (RSA) method [4].

Meanwhile, to improve the utilization of the spectrum resources, flexible-grid elastic optical network (EON) serving as the SONs has been considered as a promising enabler to satisfy the ever-increasing spectrum demand [5]. It allows the optical spectra to be allocated at the finer granularity of a few gigahertz (e.g. 12.5 GHz), which facilitates agile spectrum management in optical layer. In the EONs, a bandwidth variable transponder (BVT) is designed as a single-flow transponder (TP) in the earlier stage, which is called as ''non-sliceable TP (NS-BVT)''. It is used for elastic lightpath provisioning [6]. Hence, a BVT is only responsible for transmitting/receiving one optical flow (i.e., lightpath). Since most NS-BVTs are built with a maximal transmission rate to satisfy future demands, a NS-BVT may work inefficiently when transmission rate of the traffic is small, which results in a significant waste of resources and a large amount of unnecessary energy eventually. To further improve the resource utilization and the flexibility of the TP, sliceable bandwidth-variable transponder (SBVT) has been proposed [7]. Thus, a physical SBVT can be logically sliced into multiple sub-TPs, each of which can set up an independent lightpath for a virtual connection without electrical processing at intermediate nodes. In this paper, the SBVT-enabled EONs are assumed. Thus, multiple sub-TP channels can be ''groomed'' optically onto one physical TP, which would greatly reduce the number of active SBVTs. The outstanding feature of the SBVT can be utilized for TP energy-saving. In the paper, the two terms ''SBVT'' and ''sliceable-TP'' can be used interchangeably.

As we know, the traditional VONE scheme may lead to lower resource utilization. On one hand, a large amount of idle computing resources exist in each DCs attached with the SN, which leads to a lower DC utilization. On the other hand, much transmission resources within the TPs have not been used fully. *It is worth noting that these idle resources in the active state cause serious energy waste*.

In our preliminary work [8], we proposed a novel energy-efficient VONE scheme over EONs under dynamic (online) scenario. In this paper, we extend the previous work and further investigate the performance of both the online and offline EA-VONE problem in EONs. To the best of our knowledge, we are the first to come up with the scheme that considering both the TP reusability and the DC consolidation for reducing power consumption. As for the offline EA-VONE problem, an energy-minimized traffic-grooming-enabled integer linear programming (ILP) model is developed to obtain the optimal solution. Due to the non-scalability of the ILP model, two heuristic offline and online algorithms for the EA-VONE are designed by using proposed energy-saving schemes. Specifically, the DC-EA scheme only considers the energy-saving (ES) policy for the DCs; while the DC&TP-EA scheme simultaneously considers the EA policies for both the DCs and TPs. In the process of the node mapping, we try to embed VNs onto those active SNs that are serving other existing VON requests and turn as many idle DCs as possible into sleep mode without affecting the performance of the VONs. During the link mapping, we try to reduce the number of active SBVTs by using the optical traffic grooming technique, to save TP power consumption. In other words, we try to switch off as many active resources (i.e., DCs and TPs) as possible to minimize the energy consumption. Hence, the active resources in the SON can be dynamically dimensioned for current traffic demand rather than for peak demand. Extensive simulation results are obtained in terms of the power consumption, the resource utilization, and the request blocking probability. The simulation results show that our proposed EA-VONE algorithm significantly reduces the power consumption, and improves the resource utilization of the DCs, TPs and network links, while keeping almost same request blocking probability as that of the benchmark traffic-balancing (TB) scheme, which just focus on the performance improvement of the blocking probability.

The paper is organized as follows. Section II surveys the related works. Section III formulates the VONE problem and establishes a complete mathematical model for SON, VON request, and network power consumption. In section IV, an energy-minimized ILP model is presented. In section V, the static (offline) and dynamic (online) EA-VONE algorithms are designed, and the time complexities of the proposed algorithms are analyzed. Extensive simulation results are obtained in section VI. We finally conclude the paper in Section VII.

## II. RELATED WORK

### A. EXITING ENERGY EFFICIENT VNE SCHEME

In electrical networks, there are many studies on Virtual Network Embedding (VNE) [5], [9]–[11]. Since the power consumption of the network resources cannot change with the traffic loads, a direct way to reduce the power consumption is to design a power-variable network element for adapting the varying traffic loads. An energy-efficient VNE heuristic algorithm was designed in [5], which exploit the power-varying diversity of the physical nodes and adopt multi-attribute node ranking method to minimize the power consumption for high-revenue SONs. Another very effective way to reduce the power consumption is to turn all the possible idle resources in SON into sleep mode or even switch off them as many as possible without affecting the usability of the SON. In [9], authors introduced the virtual network embedding energy aware problem (VNE-EA) by means of resource consolidation, where the adopted policy was to allocate the set of virtual network requests in a small

set of substrate node and links (i.e, active resources), and proposed a Mixed Integer Program (MIP) to optimally solve it. The authors in [10], [11] first proposed an energy cost model and formulated the energy-aware VNE problem as an integer linear programming (ILP) problem. And two VNE algorithms were designed to reduce the energy cost while keeping nearly the same revenue so as to maximize the profit for the ISPs. However, the above VNE schemes just focus on the energy-saving of the DCs (that are attached with the SNs) via the DC resource consolidation method, but does not involve the energy-saving of the TPs within the SNs. And, these VNE schemes are not realized in the optical networks, since they do not consider the spectrum resource allocation. Some recent studies [12], [13] have suggested that optical network virtualization over flexible-grid EONs can be more flexible and efficient. But these works do not consider the energy-saving issue for VONE.

### B. OPTICAL TRAFFIC GROOMING STRATEGY

Optical traffic grooming was viewed as an effective energysaving strategy by provisioning multiple lightpaths onto a multi-flow TP (i.e., sliceableTP) [6], where each optical flow (i.e., lightpath) connects a source-destination pair all optically. The authors in [14] proposed a time-aware traffic-grooming policy for *lightpath provisioning* to reduce energy consumption and designed a spectrum reservation scheme to improve the utilization of TPs in EONs. The work in [15] investigated the energy efficiency of the static *lightpath provisioning* in IP-over-EON with sliceable TPs. Network operators can allocate a sub-TP to a lightpath, benefited from flexible optical-layer bypass of sliceable TPs. In [6], the authors studied energy-efficient traffic grooming with three types of elastic optical TP with the diffident levels of the slice ability and came to the conclusion that significant reduction in energy consumption was achievable by using full sliceable TPs. However, the above works just considered the energy-saving of the *lightpath provisioning* via optical traffic grooming within sliceable TPs. We first introduce the optical traffic grooming technique into the *VON embedding* for the sliceableTP energy-saving.

In our proposed EA-VONE, for the node mapping, we try to map VNs on active SNs, where DC has been turned on, and meanwhile switch off as many idle DCs as possible. During the link mapping, we make full use of the capacity of the sliceable TP by using optical traffic grooming technique, to minimize the number of the activated TPs. To the best of our knowledge, we are the first to propose the novel scheme that considering both the sliceable-TP reusability and the DC consolidation to reduce power consumption of the VONE scheme over the flexible-grid optical networks (i.e, EONs)

## III. PROBLEM FORMULATION

### A. VONE MODELS

As mentioned in literature [16], DCs are built very close to SNs to benefit from the large bandwidth capacities available from such SNs. In this paper, we assume that a SN includes a core optical switch (i.e., optical cross connector, OXC) and a DC. Thus, the CPU computing resources within the DC can be also viewed as the CPU resources of the corresponding SN. When the DC in a SN is turned on, the SN can be treated to be active; otherwise, it is inactive.

1) *Substrate Optical Network (SON):* It can be modeled as an undirected graph, denoted as $G^s(N^s, L^s)$, where $N^s$ is the set of SNs and $L^s$ is the set of substrate fiber links (SFLs). Each SN $n^s \in N^s$ has a total CPU computing capacity of $C(n^s)$ and the available CPU computing capacity of $c(n^s)$ $(c(n^s) \leq C(n^s))$. The total bandwidth of each SFL $l^s \in L^s$ is described to be the total number $FS^s$ of frequency slots (FSs) that a SFL $l^s \in L^s$ can accommodate. We define a bit-mask $b^s_{l^s}$ with the length of $FS^s$. When $b^s_{l^s}[i] = 1$, the $i$-th slot on the link $l^s$ is occupied, otherwise $b^s_{l^s}[i] = 0$.
2) *VON Requests:* The $i$-th VON request can also be modeled as an undirected graph $g^{vi}(N^{vi}, L^{vi})$. For the $i$-th VON $g^{vi} \in G^v$, $N^{vi}$ is the set of all VNs, and $L^{vi}$ represents the set of all VOLs. We use notation $c(n^{vi})$ to denote the required CPU computing capacity of the VN $n^{vi} \in N^{vi}$. The required bandwidth of the $i$-th VON request can be given directly in terms of the required FSs $fs(g^{vi})$.

### B. TRANSPARENT VONE PROCEDURE

When a VON request arrives, a VONE procedure selects a unique SN with enough CPU computing resources for each VN to satisfy its computing requirements. Note that the different VNs in a VON request are mapped into the different SNs, which is a common requirement for the VONE [11]–[13]. After all VNs are provisioned into the SON, the VONE procedure starts the link mapping, which needs to select SFLs that compose lightpaths to accommodate the VOLs. In this study, we only consider the transparent VONE, because that no all-optical or O/E/O spectrum converters are assumed in the SON. For transparent VONE, all the VOLs in a VON are assumed to occupy the same spectrum slots on SFLs with spectrum continuity and contiguity constraints. In other words, only when the block of one or more FSs that are available in the spectrum domain has the same in terms of indices, the FS block can be allocated to any VOL in a VON request.

Fig. 1(b) shows the VONE procedure over sliceable-TP-enabled EONs with geographically distributed DCs. A VON request is shown in Fig. 1(a). The values in the boxes around the VNs are the required amount of the CPU computing resources in this SN, and the numbers on the VOLs are the number of required FSs. After successfully embedding the VON request, an illustration of the transparent VONE procedure in the EON is shown in Fig. 1(b). The node mapping is [a $\rightarrow$ A, b $\rightarrow$ E, c $\rightarrow$ D]. The filled circle around each DC represents the computing resources usage of the DC. In the filled circle, the green and red fans respectively represent the

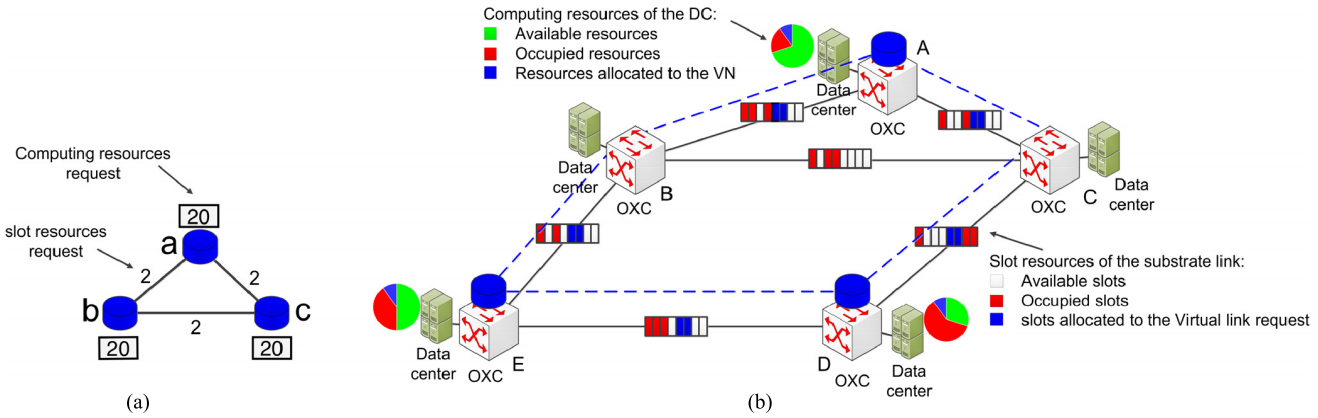


**FIGURE 1.** Illustration of the transparent VONE procedure. (a) VON request. (b) Substrate network.

available and occupied computing resources, while the blue fan denotes the allocated computing resources to the VN. The link mapping is [(a, b) → (A, B, E), (a, c) → (A, C, D), (b, c) → (E, D)]. The red boxes on the SFLs indicate the already- occupied FSs of the SFL and the blue boxes represent the FS resources allocated to VOL requests. The available slots are represented by the blank box in Fig. 1(b).

### C. POWER CONSUMPTION MODEL

In the paper, the overall power consumption of the SON mainly considers the power consumption of both the DCs and the sliceable-TPs. As discussed in [16], the CPU utilization of computing resource in a DC is the main contributor to the variation in the power consumption of a DC. Therefore, when calculating the power consumption of a DC, our efforts in the paper are restricted to the power consumed in the CPU resources of the DC. Thus, we consider the DC power profile shown in Fig. 2, which involves only the power consumption due to the CPU resources Hence, the power consumption for a DC can be defined as follows:

$$P_{DC} = \begin{cases} P_{idle} + P_l \cdot \rho, & \text{DC } \textit{is the} \text{ ON } \textit{state} \\ 0, & \text{DC } \textit{is the} \text{ OFF } \textit{state}, \end{cases} \quad (1)$$

where $P_{idle}$ is the idle power consumption of an activated DC for cooling, lighting and power supply units losses, in the case that there is no traffic load. We define that $P_{\max}$ is the maximum power when the DC is serving at the maximum traffic load Thus, $P_l = P_{\max} - P_{idle}$ denotes the power proportion factor of the DC, concerning the traffic load $\rho$ (i.e., $0 \le \rho \le 1$). Note that the traffic load here can be regarded as the CPU computing load, since both loads are of proportional relation. Hence, the newlyincreased power consumption of mapping the VN $n^v$ to the SN $n^s$ can be calculated as follows:

$$\Delta P_{DC} = \begin{cases} P_{idle} + P_l \cdot \dfrac{c\,(n^v)}{C\,(n^s)}, & \text{when the } \textit{DC was} \text{ in } \textit{OFF state} \\ P_l \cdot \dfrac{c\,(n^v)}{C\,(n^s)}, & \text{when the } \textit{DC was} \text{ in } \textit{ON state}, \end{cases} \quad (2)$$

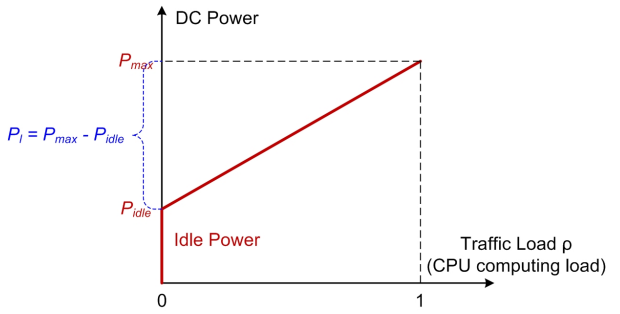


**FIGURE 2.** Illustration of the DC power versus traffic load [16].

where the $c\,(n^v)/C\,(n^s)$ represents the CPU computing load of the SN $n^s \in N^s$, which can be also viewed as the traffic load $\rho$ of the SN.

As for a sliceable-TP, the power consumption can be expressed as:

$$P_{tp} = P_{overhead} + \eta \times TR \quad (3)$$

The $TR$ denotes the TP transmission rate (TR) in term of Gbit/s and $P_{overhead}$ is the overhead power consumption in the unit of watt [6]. The $\eta$ is a power coefficient in the unit of watt/ Gbit/s. Note that the $TR$ is the sum of transmission rates of all working sub-TPs within the TP. As long as the TP is in the active state, its overhead power consumption is an indispensable part even though its transmission rate is zero. By changing the parameter values of the $P_{overhead}$ and the power coefficient $\eta$ in Eq. (3), we can evaluate the power of the different TP technologies in a unified manner. The TP model shown in Eq. (3) scales linearly with transmission rate, after mapping a VOL request on the SFLs, so the newlyincreased TP power consumption for the VOL mapping can be calculated as follows:

$$\Delta P_{tp} = \begin{cases} P_{overhead} + \eta \times tr\,(l^v), & \text{if } \textit{TP was active} \\ \eta \times tr\,(l^v), & \text{if } \textit{TP was inactive} \end{cases} \quad (4)$$

where $tr\,(l^v)$ denotes the transmission rate (i.e., bandwidth requirements) of the VOL $l^v$. We assume that one FS can carry $C_{FS} = 12.5\ Gbit/s$ signal when the modulation-format is binary phase shift keying (BPSK) [13]. Thus, the bandwidth requirement of the VOL $l^v$ equals to $fs\,(l^v) \times C_{FS}$, where $C_{FS}$

is the bandwidth capacity of a single FS, and $fs(l^v)$ denotes the required FSs of the VOL $l^v$ for the $i$-th VON request $g^v$. For transparent VON, $fs(l^v) = fs(g^v)$, $l^v \in g^v$ can always hold.

### D. ENERGY-SAVING OBJECTIVE

The objective of the EA-VONE problem in our study is to minimize the power consumption of the entire SON, including the power consumption of the DCs and sliceable- TPs. From the above power consumption model, we can find that the following two factors would seriously affect the energy saving performance: i) the idle power consumption $P_{idle}$ of DCs, and ii) the overhead power consumption $P_{overhead}$ of TPs, because that these power consumption values are irrelevant to the traffic load. Hence, eliminating power waste as much as possible from the above two factors will be helpful for us to design an energyefficient VONE

## IV. ILP FORMULATION

In this section, we formulate a novel ILP model for the transparent VONE over the sliceable-TP-enabled EONs, with the energy-saving consideration for the SON. The novelties of the ILP model are that: 1) traffic-grooming strategy is applied into the ILP model, with which the required SCs of the multiple VOLs can be optically groomed into single TP; and 2) the objective of minimizing both DCs and TPs power in a combined manner is original.

### A. PARAMETERS

1) $G^s(N^s, L^s)$: The substrate EON (i.e., SON) infrastructure.
2) $g^{vi}\left(N^{vi}, L^{vi}\right)$: The $i$-th VON request $g^{vi} \in G^v$.
3) $C(n^s)$: Total CPU computing capacity of each SN $n^s \in N^s$
4) $SC\left(tp_{n^s}^k\right)$: Total capacity of subcarriers (SC) of the $k$-th TP in the SN $n^s$.
5) $c\left(n^{vi}\right)$: CPU computing resource requirement of the VN $n^{vi} \in N^{vi}$ of the $i$-th VON request $g^{vi} \in G^v$.
6) $fs\left(g^{vi}\right)$: The bandwidth demand measured in the number of FSs for the VOLs $l^{vi} \in L^{vi}$ of the $i$-th VON request $g^{vi} \in G^v$.
7) $tr\left(l^{vi}\right)$: Transmission rate of the TP for the VOLs $l^{vi} \in L^{vi}$ of the $i$-th VON request $g^{vi}$ according to the required $fs\left(l^{vi}\right)$ and a specific modulation format. In this work, one FS is assumed to carry $C_{FS} = 12.5\ Gbit/s$ with the modulation-format of BPSK. Thus, $tr\left(l^{vi}\right) = fs\left(l^{vi}\right) \times C_{FS}$.
8) $Len(u^s, w^s)$: The fiber length of the link $(u^s, w^s) \in L^s$.
9) $|G^v|$: The total number of VON requests.
10) $F$: A large value.

### B. VARIABLES

1) $vnsntp\left(n^{vi}, tp_{n^s}^k\right)$: A boolean variable that equals 1 if the VN $n^{vi}$ of the $i$-th VON request $g^{vi}$ is mapped to the $k$-th TP within the SN $n^s$.
2) $vnsn\left(n^{vi}, n^s\right)$: A boolean variable that equals 1 if the VN of the i-th VON request is mapped to the SN $n^s$.
3) $volsfl\left((u^{vi}, w^{vi}), (u^s, w^s)\right)$: A boolean variable that equals 1 if the VOL $\left(u^{vi}, w^{vi}\right)$ of the $i$-th VON request $g^{vi}$ is mapped onto a lightpath including the SFL $(u^s, w^s)$.
4) $\xi_{sc}\left(g^{vi}, g^{vj}\right)$: A boolean variable that takes the value of zero if the subcarrier index $E_{sc}\left(g^{vj}\right)$ in the $k$-th TP in the SN $n^s$ that the $j$-th VON request used is smaller than the subcarrier index $S_{sc}\left(g^{vi}\right)$ in the $k$-th TP in the SN $n^s$ that the $i$-th VON request used. This notation makes sense only when two different VON request share common TP within a SN.
5) $\delta_{fs}\left(g^{vi}, g^{vj}\right)$: A boolean variable that takes the value of zero if the slot index $E_{fs}\left(g^{vj}\right)$ of the $j$-th VON request is smaller than the starting slot index $S_{fs}\left(g^{vi}\right)$ of the $i$-th VON request. This notation makes sense only when two different VON request share common link(s).
6) $\psi\left(tp_{n^s}^k\right)$: A boolean variable that equals 1 if the $k$-th TP in the SN $n^s$ is activated during the simulation period.
7) $\psi\left(dc_{n^s}\right)$: A boolean variable that equals 1 if the DC attached with the SN $n^s$ is turned on during the simulation period.
8) $S_{fs}\left(g^{vi}\right)$: An integer variable that denotes the starting FS index of the $i$-th VON request $g^{vi}$.
9) $E_{fs}\left(g^{vi}\right)$: An integer variable that denotes the ending FS index of the $i$-th VON request $g^{vi}$.
10) $S_{sc}\left(g^{vi}, tp_{n^s}^k\right)$: An integer variable that denotes the starting SC index of the $k$-th TP in SN $n^s$ that $i$-th VON request $g^{vi}$ occupied.
11) $E_{sc}\left(g^{vi}, tp_{n^s}^k\right)$: An integer variable that denotes the ending SC index of $k$-th TP in SN $n^s$ that the $i$-th VON request $g^{vi}$ occupied.

### C. OBJECTIVE

The objective function of this ILP model minimizes the average total power consumption for all accommodated VON requests as shown in Eq. (5), including the power consumptions of the TPs, DCs and erbium-doped fiber amplifiers (EDFAs) in the entire network. The EDFA is used for signal power compensation along the fiber links Each element of the power consumption is mathematically defined in Eq. (5)-(8), as shown at the top of the next page. Note that in Eq. (8), an EDFA is placed every 80km fiber link to improve the transmission quality, and its power consumption is 8W [3].

### D. CONSTRAINTS

#### 1) NODE MAPPING CONSTRAINTS

$$\sum_{n^s \in N^s} \sum_{alltp_{n^s}^k} vnsntp\left(n^{vi}, tp_{n^s}^k\right) = 1, \quad \forall n^{vi} \in N^{vi},\ \forall g^{vi} \in G^v \tag{9}$$

$$\sum_{n^{vi} \in N^{vi}} \sum_{alltp_{n^s}^k} vnsntp\left(n^{vi}, tp_{n^s}^k\right) \leq 1, \quad \forall n^s \in N^s,\ \forall g^{vi} \in G^v \tag{10}$$

$$Minimize\ (P_{TP} + P_{DC} + P_{EDFA}) \tag{5}$$

$$P_{TP} = P^{TP}_{overhead} + P^{TP}_{dep} = \frac{\sum_{n^s \in N^s} \sum_{all\ tp^k_{n^s}} P_{overhead} \times \psi\left(tp^k_{n^s}\right) + \sum_{g^{vi} \in G^v} \sum_{l^{vi} \in L^{vi}} \eta \times tr\left(l^{vi}\right) \times 2}{|G^v|} \tag{6}$$

$$P_{DC} = P^{DC}_{idle} + P^{DC}_{dep} = \frac{\sum_{n^s \in N^s} P_{idle} \times \psi\left(dc_{n^s}\right) + \sum_{g^{vi} \in G^v} \sum_{n^{vi} \in N^{vi}} P_l \times c\left(n^{vi}\right)/C\left(n^s\right)}{|G^v|} \tag{7}$$

$$P_{EDFA} = \frac{\sum_{g^{vi} \in G^v} \sum_{\substack{(u^{vi}, w^{vi}) \in L^{vi} \\ (u^s, w^s) \in L^s}} \left[ \begin{array}{c} volsfl\left(\left(u^{vi}, w^{vi}\right), \left(u^s, w^s\right)\right) \\ \times Len\left(u^s, w^s\right)/80 \end{array} \right] \times 8}{|G^v|} \tag{8}$$

Equations (9) and (10) ensure that each VN in a VON request is mapped onto a unique SN and a unique TP in the mapped SN.

$$vnsn\left(n^{vi}, n^s\right) = \sum_{all tp^k_{n^s}} vnsntp\left(n^{vi}, tp^k_{n^s}\right), \quad \forall n^{vi} \in N^{vi}, \quad \forall n^s \in N^s, \ \forall g^{vi} \in G^v \tag{11}$$

Equation (11) ensures that once any TP within the SN $n^s$ is used, this SN $n^s$ will definitely be used.

$$\sum_{g^{vi} \in G^v} \sum_{n^{vi} \in N^{vi}} vnsn\left(n^{vi}, n^s\right) \times c\left(n^{vi}\right) \le C\left(n^s\right), \quad \forall n^s \in N^s \tag{12}$$

Equation (12) ensures that the embedded SN has enough computing capacity to accommodate the VNs.

### 2) SUBCARRIERS PROVISIONING CONSTRAINTS

$$\sum_{g^{vi} \in G^v} \sum_{n^{vi} \in N^{vi}} vnsntp\left(n^{vi}, tp^k_{n^s}\right) \times fs\left(l^{vi}\right) \le SC\left(tp^k_{n^s}\right), \quad \forall n^s \in N^s, \quad \forall tp^k_{n^s} \tag{13}$$

where the number of the required subcarriers in the occupied TP in the SN is equal to the required number of FSs for the VOLs $l^{vi} \in L^{vi}$ of the $i$-th VON request $g^{vi}$. Equation (13) ensures that occupied TP in the SN has enough subcarrier capacity to accommodate the VNs.

$$\xi_{sc}\left(g^{vi}, g^{vj}\right) + \xi_{sc}\left(g^{vj}, g^{vi}\right) = 1, \quad \forall g^{vi}, g^{vj} \in G^v, \ g^{vi} \ne g^{vj} \tag{14}$$

$$E_{sc}\left(g^{vj}, tp^k_{n^s}\right) - S_{sc}\left(g^{vi}, tp^k_{n^s}\right) \le F \times \left[ \begin{array}{c} \xi_{sc}\left(g^{vi}, g^{vj}\right) + 2 \\ -vnsntp\left(n^{vi}, tp^k_{n^s}\right) - vnsntp\left(n^{vj}, tp^k_{n^s}\right) \end{array} \right] - 1, \quad \forall g^{vi}, g^{vj} \in G^v, \quad g^{vi} \ne g^{vj}, \ \forall tp^k_{n^s} \quad \forall n^{vi} \in N^{vi}, \quad \forall n^{vj} \in N^{vj}, \ \forall n^s \in N^s \tag{15}$$

Equations (14) and (15) ensure that when the subcarriers (SCs) of two VON requests share common sliceable-TP in a SN, the assigned SCs for two VONs must not overlap each other. In other words, the assigned SCs of the TP for one VON can be either before or after the SCs of the TP for the other VON. Based on the above constraints, in the case that $n^{vi}$ of the VON $g^{vi}$ and $n^{vj}$ of the other VON $g^{vj}$ share a common TP in the same SN $n^s$, i.e., $vnsntp\left(n^{vi}, tp^k_{n^s}\right) = 1$, $vnsntp\left(n^{vj}, tp^k_{n^s}\right) = 1$ and $\xi_{sc}\left(g^{vi}, g^{vj}\right) = 0$, then $S_{sc}\left(g^{vi}, tp^k_{n^s}\right) \ge E_{sc}\left(g^{vj}, tp^k_{n^s}\right) + 1$ can be obtained; otherwise, the inequality (15) always holds. In summary, Eq. (14)-(15) ensure that both of the constraints of SC contiguous within each TP in the SN, and satisfy the SC non-overlap requirement for different VNs that share same TP in the same SN.

### 3) LINK MAPPING CONSTRAINTS

$$\sum_{(u^s, w^s) \in L^s} volsfl\left(\left(u^{vi}, w^{vi}\right), \left(u^s, w^s\right)\right) - \sum_{(w^s, u^s) \in L^s} volsfl\left(\left(u^{vi}, w^{vi}\right), \left(w^s, u^s\right)\right) = vnsn\left(u^{vi}, w^s\right) - vnsn\left(w^{vi}, w^s\right), \quad \forall \left(u^{vi}, w^{vi}\right) \in L^{vi}, \quad \forall w^s \in N^s \tag{16}$$

Equation (16) is the flow conservation constraint. This constraint ensures that on all the SNs, the total number of the in-flows equals to that of the out-flows, except for the embedded SNs for the end-nodes of the VOL. This ensures a unique route of the lightpath established for one specific VOL.

$$\sum_{(u^{vi}, w^{vi}) \in L^{vi}} volsfl\left(\left(u^{vi}, w^{vi}\right), \left(u^s, w^s\right)\right) = 1, \quad \forall g^{vi} \in G^v, \quad \forall \left(u^s, w^s\right) \in L^s \tag{17}$$

Equation (17) ensures that for all the VOLs in the same VON $g^{vi}$, their embedded lightpaths in the substrate EON are

link-disjoint.

$$volsfl\left(\left(u^{vi}, w^{vi}\right), \left(u^{s}, w^{s}\right)\right) = volsfl\left(\left(u^{vi}, w^{vi}\right), \left(w^{s}, u^{s}\right)\right) \quad \forall g^{vi} \in G^{v}, \forall \left(u^{s}, w^{s}\right) \in L^{s}, \quad \forall \left(u^{vi}, w^{vi}\right) \in L^{vi} \tag{18}$$

Equation (18) ensures that all the VOLs in the VON request, all the SFLs in the substrate EON are undirected.

#### 4) SPECTRUM PROVISIONING CONSTRAINTS

$$\delta_{fs}\left(g^{vi}, g^{vj}\right) + \delta_{fs}\left(g^{vj}, g^{vi}\right) = 1, \quad \forall g^{vi}, g^{vj} \in G^{v}, \quad g^{vi} \neq g^{vj} \tag{19}$$

$$E_{fs}\left(g^{vj}\right) - S_{fs}\left(g^{vi}\right) \leq F \times \begin{bmatrix} \delta_{fs}\left(g^{vi}, g^{vj}\right) + 2 \\ -volsfl\left(\left(u^{vi}, w^{vi}\right), \left(u^{s}, w^{s}\right)\right) \\ -volsfl\left(\left(u^{vj}, w^{vj}\right), \left(u^{s}, w^{s}\right)\right) \end{bmatrix} - 1, \quad \forall g^{vi}, g^{vj} \in G^{v}, \quad g^{vi} \neq g^{vj}, \ \forall \left(u^{s}, w^{s}\right) \in L^{s}, \ \forall \left(u^{vi}, w^{vi}\right) \in L^{vi} \in g^{vi}, \quad \forall \left(u^{vj}, w^{vj}\right) \in L^{vj} \in g^{vj} \tag{20}$$

Equations (19) and (20) can ensure that the spectrum of two VON requests that share the common SFL(s), the assigned FSs of one VON lightpath can be either before or after the FSs of the other VON lightpath. Based on the above constraints, if the two lightpaths VOLs $\left(u^{vi}, w^{vi}\right)$ and $\left(u^{vj}, w^{vj}\right)$ share a common link $\left(u^{s}, w^{s}\right)$, i.e., $volsfl\left(\left(u^{vi}, w^{vi}\right), \left(u^{s}, w^{s}\right)\right) = 1$, $volsfl\left(\left(u^{vj}, w^{vj}\right), \left(u^{s}, w^{s}\right)\right) = 1$ and $\delta_{fs}\left(g^{vi}, g^{vj}\right) = 0$, then we can obtain $S_{fs}\left(g^{vi}\right) \geq E_{fs}\left(g^{vj}\right) + 1$; otherwise, the inequality (20) always holds. In summary, equations (19) and (20) can ensure that both of the constraints of FS continuity and contiguous for each VOL, and satisfy the FS non-overlap requirement for two different VOLs that share common link(s).

#### 5) OTHER CONSTRAINTS

$$E_{fs}\left(g^{vi}\right) = S_{fs}\left(g^{vi}\right) + fs\left(g^{vi}\right) - 1, \quad \forall g^{vi} \in G^{v} \tag{21}$$

$$E_{sc}\left(g^{vi}, tp_{n^s}^{k}\right) = S_{sc}\left(g^{vi}, tp_{n^s}^{k}\right) + fs\left(g^{vi}\right) - 1, \quad \forall g^{vi} \in G^{v}, \quad \forall n^{s} \in N^{s}, \ \forall tp_{n^s}^{k} \tag{22}$$

Equation (21) can ensure that the ending FS index of one VON is equal to the starting slot index of the VON plus the number of FSs required by the VON request and Equation (22) ensures that the ending SC index of the occupied TP in the SN is equal to the starting SC slot index plus the number of FSs required by the VON request. Here, we assume that the number of the required SCs is equal to the number of the required FSs for the VOLs $l^{vi} \in L^{vi}$ of the VON request $g^{vi}$.

$$\psi\left(tp_{n^s}^{k}\right) = \begin{cases} 0, & \text{if } \sum_{g^{vi} \in G^{v}} \sum_{n^{vi} \in N^{vi}} vnsntp\left(n^{vi}, tp_{n^s}^{k}\right) = 0 \\ 1, & \text{if } \sum_{g^{vi} \in G^{v}} \sum_{n^{vi} \in N^{vi}} vnsntp\left(n^{vi}, tp_{n^s}^{k}\right) \geq 1, \end{cases} \quad \forall n^{s} \in N^{s}, \quad \forall tp_{n^s}^{k} \tag{23}$$

$$\psi\left(dc_{n^s}\right) = \begin{cases} 0, & \text{if } \sum_{alltp_{n^s}^{k}} \psi\left(tp_{n^s}^{k}\right) = 0 \\ 1, & \text{if } \sum_{alltp_{n^s}^{k}} \psi\left(tp_{n^s}^{k}\right) \geq 1, \end{cases} \quad \forall n^{s} \in N^{s}, \ \forall dc_{n^s} \tag{24}$$

Equation (23) is formulated to judge whether the $k$-th TP in the SN $n^s$ is activated during the simulation period. Specifically, the $k$-th TP in the SN $n^s$ is activated, as long as the $k$-th TP is used by any one VON request. Analogously, we can tell whether the DC attached with the SN $n^s$ is turned on during the simulation period by Eq. (24). The fact that any TP in the SN $n^s$ is used indicates that the DC attached with the SN $n^s$ will definitely be activated.

## V. TRANSPARENT EA-VONE ALGORITHM

As we know, the newly developed ILP model can get the optimal solution for the transparent VONE provisioning in the most compact way and obtain the minimized power consumption for the entire network. However, the high computational complexity of the ILP model limits its scalability to address very large network instances, and it can only be applied to small-scale problems. Therefore, in this section, we proposed time-efficient heuristic algorithms for the transparent EA-VONE over the sliceable-TP-enabled EONs.

To reduce unnecessary power consumption resulting from the two factors as mentioned in Section III.D, we consider the energy saving of both the DCs and TPs for transparent EA-VONE over EONs in a dynamic scenario. Specifically, we introduce the DC node consolidation technique into the node mapping algorithm for DC energy-saving; meanwhile we will make full use of the capacity of the sliceable-TPs equipped within each SN by considering optical traffic grooming strategy during the link mapping.

### A. LAG APPROACH

For clarity, a layered auxiliary graph (LAG) approach was introduced [13]. It transforms the SON into several layered sub-graphs, according to the bandwidth requirement of the VON request. Generally, when a VON request arrives, the LAG approach first calculates the required FSs $fs\left(g^{vi}\right)$, according to the bandwidth requirement $bw\left(g^{vi}\right)$ of the VON request and a specific modulation format. Note that the number of required FSs for each VON request is given out directly in this paper. Then, we decompose the SON topology into $\left(FS^{s} - fs\left(g^{vi}\right) + 1\right)$ layers by scanning the spectrum utilization of all the $FS^{s}$ slots for each SFL ($l^{s} \in L^{s}$). For the $i$-th layer, the LAG checks whether the contiguous slot-block covering $i$-th to $(i + fs\left(g^{vi}\right) - 1)$-th FS exists on each SFL. If the contiguous slot-block exists on an SFL $l^{s}$, the $l^{s}$ will be inserted into the $i$-th layer. After all eligible links have been added to the layer, the $i$-th layer is completed, which is denoted as $G_{i}^{sub}$. By analogy, the LAG routine finishes until all layers are constructed.

**Algorithm 1** Node Mapping

**Input:** $G^s$, $g^{vl}$
**Output:** VON node mapping status $F$ and SON $G^s$
1 Calculate $h(n^s)$ for each $n^s \in E^s$ in $G^s$;
2 Calculate $h(n^v)$ for each $n^v \in N^v$ in $g^{vl}$;
3 **For** all VNs $n^v$ in descending order of their $h(n^v)$
4 $F$ = FAILED;
5 Set a flag bit $K(n^s) = 1$ for each $n^s \in E^s$;
6 **For** all active SNs $n^s$ in descending order of their $h(n^s)$
7 **If** $c(n^s) \geq c(n^v)$ **AND** $d(n^s) \geq d(n^v)$ **AND** $K(n^s) = 1$ **then**
8 Map $n^v$ onto $n^s$;
9 $K(n^s) = 0$;
10 $F$ = SUCCEED and break;
11 **End**
13 **End**
14 **If** $F ==$ FAILED **then**
15 **For** all inactive SNs $n^s$ in descending order of $h(n^s)$
16 **If** $c(n^s) \geq c(n^v)$ **AND** $d(n^s) \geq d(n^v)$ **AND** $K(n^s) = 1$ **then**
17 Map $n^v$ onto $n^s$;
18 $K(n^s) = 0$;
19 $F$ = SUCCEED;
20 break;
21 **End**
22 **End**
23 **End**
24 **End**
25 **Return** $F$;

### B. NODE MAPPING

The algorithm 1 gives out the details of the node mapping. First, two important parameters (i.e., $h(n^s)$ and $h(n^v)$) are calculated for each SN $n^s \in N^s$ and each VN $n^v \in N^v$, respectively. These parameters are defined in Eq. (25) and Eq. (26), respectively. Note that for a SN $n^s \in N^s$, we not only need to make sure that there is enough computing resource available in the DC, but also should consider its connectivity with the adjacent SNs to prepare for the subsequent link mapping. Hence, according to the literature [19], the local resource capacity (LRC) of a SN is introduced, which includes both the computing and the network link resources. In other words, the local information of a SN $n^s$ contains its available computing resource capacity $c(n^s)$ within its DC and its node degree $d(n^s)$. We define the LRC of a SN as follows:

$$h\left(n^s\right) = c\left(n^s\right) \cdot d\left(n^s\right) \tag{25}$$

Intuitively, a larger value of $h(n^s)$ means that the SN $n^s$ has more computing resource and physical links attached Similarly, for a VN $n^v$ of a VON request, its required resource capacity (RRC) can be calculated as:

$$h\left(n^v\right) = c\left(n^v\right) \cdot d\left(n^v\right) \tag{26}$$

where $d(n^v)$ denotes the node degree of the VN $n^v$ in the VON request.

As mentioned in section III.D, to alleviate idle power consumption of DCs as much as possible, we design the node mapping algorithm which seeks to map VNs as many as possible onto existing active SNs to minimize the number of active SNs. Only if all existing active SNs can't accommodate the new VN, a new DC attached with a new SN should be activated (see more in algorithm 1). Note that the flag bit $K(n^s)$ in line 5 of the algorithm 1 is used to ensure that any VN in a VON request must be mapped into a unique SN. Thus, for a VON request, if a SN is selected, the SN becomes no longer available and let $K(n^s) = 0$.

Note that in the node mapping, only the resource capacity is considered, but its impact (e.g., distance between nodes) on the link mapping is not involved, which is out of the scope of this paper

### C. LINK MAPPING

After all the VNs are embedded successfully into SONs, we can step into the link mapping. Similar to routing and spectrum assignment (RSA) problem [21], each link mapping needs to decide how to route each VOL onto the SFLs and how to assign a contiguous slot-block to each SFL under the spectrum contiguous and continuity constraints. The details of the link mapping are shown in the algorithm 2.

Generally, the algorithm 2 has two steps in turn: i) setting up lightpaths for all VOLs in a VON request with the aid of the LAG approach, and ii) performing optical traffic grooming using sliceable-TPs for all established lightpaths.

In Step 1: In the ascending order of the index of the spectrum slots, the proposed link mapping algorithm sets up a lightpath for each VOL in a given VON using the shortest-path routing in a certain LAG. Since the construction principle of the LAG makes sure that both the routing path and the FS' on them are available for a VOL, we achieve integrated RSA. After a VOL can be mapped into the LAG, the corresponding links in the lightpath are removed from the LAG. The procedure is done in turn until the lightpaths of all VOLs of this VON request have been set up successfully in this LAG. Otherwise, the next LAG would be tried for the provisioning of all the VOLs in a given VON.

In Step 2: To reduce the power waste as much as possible due to the overhead power consumption of TPs, we will use optical traffic grooming strategy to aggregate multiple optical flows into one physical SBVT as much as possible, in order to lower the amount of the activated TPs. For all established lightpaths in the above step, we provision the sub-TP resources one-by-one. For a new VOL connection request, there are three possible operations as follows.

*Operation 1:* Establish a new lightpath using a sub-TP both in its source and destination nodes by grooming the VOL request onto two existing activated SBVTs.

*Operation 2:* Establish a new lightpath using a sub-TP in either its source or destination node by grooming the VOL request onto an existing activated SBVT.

**Algorithm 2** Link Mapping

**Input:** SON $G^s$ after node mapping and $g^{vl}$
**Output:** VON mapping state $VS$, $G^s$ after link mapping

Get lightpath demands $t(s, d, fs(g^{vl}))$ for all VOLs in the VON $g^{vl}$ and store them in group $Q$;
Create a group $R$ to store the RSA information $RSA(t(s, d, fs(g^{vl})))$ for each VOL request $t(s, d, fs(g^{vl}))$;
$VS$ = FAILED;
// Step 1: setting up lightpaths for all VOLs in a VON
**For** $i = 1$ to $FS^s - fs(g^{vl}) + 1$
  **For** each $t(s, d, fs(g^{vl}))$ in group Q
    build the $i$-th LAG $GG^{ub}$;
    find the shortest path from $s$ to $d$ in $G_l^{sub}$ for each $t(s, d, fs(g^{vl}))$;
    **If** the path in $G_l^{sub}$ can be found **then**
      generate a lightpath $RSA(t(s, d, fs(g^{vl})))$ and store it in group $R$;
      remove all SFLs of the path in $GG^{ub}$;
    **Else**
      Clear out the group $R$;
      break;
  **End**
  **If** the group $R$ is not Null **then**
    $VS$ = SUCCEED and break;
**End**
// Step 2: performing optical traffic grooming using SBVT for all established lightpaths
**For** all lightpaths $RSA(t(s, d, fs(g^{vl})))$ in group $R$
  perform operation 1;
  **If** operation 1 failed **then**
    perform operation 2;
  **If** operation 1 or 2 succeed then
    Update TP status including capacity and number of activated sub-TPs and capacity of all SFLs in $G^s$;
  **Else**
    **do** operation 3 and update TP status and capacity of all SFLs in $G^s$;
  **Return** $G^s$ after mapping $g^{vl}$ successfully;
**End**
**Return** $VS$;

*Operation 3:* Establish a new lightpath using two new- activated SBVTs both in its source and destination nodes.

Fig. 3 indicates the examples of the link mapping for three VOLs in a VON request using the two different types of TPs (i.e., SBVT, NS-BVT). Fig. 3(a) gives out a VON request with three VNs and three VOLs, where the numbers in the boxes around the VNs are their required CPU computing resource and the values on the VOLs are the required slots FSs. The underlying SON is assumed to be a three-node network with bidirectional links. Thus, the node mapping is [a → A, b → B, c → C] and the link mapping is [(a, b) → (A, B), (a, c) → (A, C), (b, c) → (B, C)] using algorithm 1 and 2, respectively. In Fig. 3(b) and Fig. 3(c), the black boxes indicate the unavailability slots within the SBVT; and the black arrowed lines represent the existing lightpaths. Note that we only focus on the utilization of TPs for VOL requests in Fig. 3. We assume that there are eight subcarriers in each SBVT.

In Fig. 3(b), for the VOL request [(a, c) → (A, C)], a new lightpath can be established successfully using *Operation 1*. Four free subcarriers within TP-A1 in node A and four free subcarriers within TP-C1 in node C can be used by optical traffic grooming for the VOL request. For the VOL request [(b, c) → (B, C)], we can use *Operation 2* to groom the request onto subcarriers in an existing activated TP-B1 in the source node, while a new SBVT has to be activated at destination node C. For the VOL request [(a, b) → (A, B)], because no free subcarriers are available under the spectrum constraints, we must adopt *Operation 3* to activate two new SBVTs both in the source and destination nodes, for establishing the new VOL request. Therefore, we just need to activate three new SBVTs for the VON request, by using optical traffic grooming. We can also find from Fig. 3(c) that without optical traffic grooming, each SN activates one more NS-BVT in each node, compared with the scenario in Fig. 3(b). It is because that a NS-BVT is a single-flow TP, and we have to turn on a new TP for each VOL request both in source and destination nodes. Moreover, the transmission capacity in each node cannot be fully utilized, which may turn out to be a waste of resources.

### D. TIME COMPLEXITY ANALYSIS

The time complexities of the proposed algorithms are analyzed as follows.

In the LAG algorithm, the $(FS^s - fs\left(g^{vi}\right) + 1)$ sub-layers are created, and hence the time complexity of the LAG algorithm is $O((FS^s - fs\left(g^{vi}\right) + 1)\,|L^s|)$.

For the node mapping, the time complexity of sorting SNs and VNs are $O(|N^v|^2)$ and $O(|N^s|^2)$, respectively. Thus, the overall time complexity of the node mapping algorithm is $O(|N^s|^2 + |N^v|^2 + |N^s|\,|N^v|)$.

For link mapping, the complexity of the Dijkstra algorithm on a sub-layer is $O(|N^s| + |N^s|\,(|N^s| - 1) + |N^s| \log 2\,|N^s|)$ [4], and the time complexity of performing traffic grooming is $O(T\,|N^v|)$, where $T$ denotes the total number of subcarriers within a SBVT. Thus the overall time complexity of the link mapping algorithm is

$$O(|L^v| \times (|N^s| + |N^s|(|N^s| - 1) + |N^s| \log 2|N^s| + T|N^v|)).$$

### E. OVERALL HERRISTIC EA-VONE ALGORITHMS

Based on the proposed algorithms, we design the overall energy efficient VONE algorithms under both offline and online scenarios.

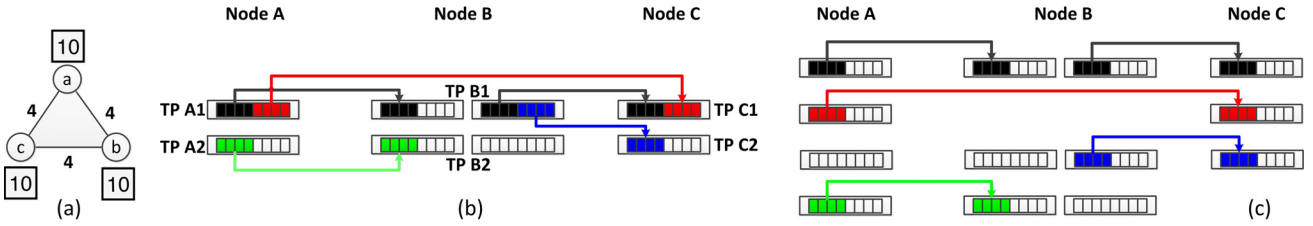


**FIGURE 3.** (a) VON request with three VOLs, (b) optical traffic grooming using SBVT, and (c) no optical traffic grooming with NS-BVT.

**Algorithm 3** Overall Offline EA-VONE Algorithm

```
Sort all requests in descending order based on bw(g^vl)
For each VON request
    Get its bandwidth requirement bw(g^vl);
    Obtain fs(g^vl) with bw(g^vl) and modulation format;
    do node mapping with Algorithm 1;
    If F == SUCCEED then
        do link mapping with Algorithm 2;
    Else
        Mark the VON request g^vl as blocked;
        VS = FAILED;
    End
Return VS;
```

**Algorithm 4** Overall Online EA-VONE Algorithm

**Input:** Substrate network $G^s$, the VON request $g^{vl}$
**Output:** VONE status $VS$

```
Get the arrival time AT(g^vl) of the VON request g^vl;
T_current = AT(g^vl);
Get bandwidth requirement bw(g^vl) of the VON request;
Calculate fs(g^vl) with bw(g^vl) and modulation format;
If V_provisioned is not NULL then
    For each g^vj ∈ V_provisioned
        If AT(g^vj) + ΔT(g^vj) ≤ T_current then
            Release the occupied resources and remove the VON request g^vj from the set V_provisioned;
    End
End
do node mapping with Algorithm 1;
If F == SUCCEED then
    do link mapping with Algorithm 2;
    If VS == SUCCEED then
        g^vl is put into the set V_provisioned, and its status is set to be waiting for releasing at time AT(g^vl)+ΔT(g^vl);
    End
Else VS == FAILED;
End
Return VS;
```

#### 1) OFFLINE (STATIC) HEURISTIC EA-VONE ALGORITHM

For the offline (static) scenario, we assume that all the VON requests with specific bandwidth requirement $bw\left(g^{vi}\right)$ are generated randomly in advance. These VON requests will be fulfilled one by one in the order of the descending order of their $bw\left(g^{vi}\right)$. Each time a VON is provisioned successfully, the DCs attached to the corresponding SNs, the SC resources within the corresponding TPs and the FSs on corresponding SFLs are occupied, respectively. More details can be seen in Algorithm 3.

#### 2) ONLINE (DYNAMIC) HEURISTIC EA-VONE ALGORITHM

For the online scenario, each VON request undergoes a birth-and-death process, i.e., arriving sequentially and randomly, holding for a certain time, and finally departing, releasing the corresponding occupied resources. Specifically, the arrival time and lifetime of each VON request are denoted as $AT\left(g^{vi}\right)$ and $\Delta T\left(g^{vi}\right)$. The initial time point is defined as the starting time of the first VON request to arrive, and the current time $T_{current}$ is initialed to be the $T_{initial}$. The set of all the already provisioned VON requests are denoted as $V_{provisioned}$. Once the $i$-th VON request arrives at the time $AT\left(g^{vi}\right)$, we assume the VONE process will be executed immediately. Before the new VON request is provisioned, the algorithm will automatically check whether it is time to release those already provisioned VON requests before $(i+1)$ VON request arrives. If any of these VON requests has a lifetime that is about to expire, the occupied resources will be released after the lifetime of this VON request. Then the $i$-th VON request starts to be provisioned. If it is provisioned successfully, the status of this VON request will be set as ''waiting for releasing''.

## VI. PROBLEM EVALUATIONS

In this section, we design simulations to evaluate the performance of the proposed online and offline EA-VONE algorithms. During the simulations, we assume that the number $n$ of VNs in each VON request is randomly taken in an integer set [3], [4] and the probability that a VN-pair is directly connected equals to 0.5. As a result, the average number of

**TABLE 1. Simulation parameters.**

| SON | Five-Node Topology | DT Topology | VON requests | |
|---|---|---|---|---|
| Number of SNs | 5 | 14 | Number of VNs in a VON | [3, 4] |
| Number of SFLs | 6 | 23 | Number of VOLs in a VON | $\frac{n(n-1)}{4}$ |
| Computing Capacity of SN | 1000 units | 1000 units | Computing Requirement of VN | [2, 20] units |
| Bandwidth Capacity of SFL | 160 slots | 320 slots | Bandwidth Requirement of VOL | [1, 8] slots |

VOLs in a VON is $n(n-1)/4$. Key simulation parameters are shown in Table 1.

### A. SIMULATION SETUP

For the offline (static) scenario, we consider the average power consumption per accommodated VON to evaluate the performance of the ILP model and our proposed scheme in the simple five-node network, as shown in Fig. 3(a). We make the assumption that $P_{overhead} = 91.333$W and $\eta = 1.683$W/Gbit/s according to [6]. It is assumed that each DC in the SN contains 50 Dell Power Edge R720 Servers [22], each with idle power rated at 112W and 365W at full load. Thus, the total idle power of an entire DC is 5600W (i.e., $50 \times 112$W). We also assume that whole CPU capacity of a DC is set to be 1000 units. The required computing resource $c(n^v)$ of the VN $n^v \in N^v$ is assumed to be uniformly distributed between 2 and 20 units. Bandwidth capacity of each SFL is 160 FSs and the number of required slots of each VOL is evenly distributed between 1 and 8 slots. Meanwhile, one FS is assumed to occupy 12.5GHz spectrum block. For simplicity, the modulation format of BPSK (Binary Phase Shift Keying) is set for all VOLs, and thus a single BPSK subcarrier can afford 12.5Gbps capacity. We consider 100Gbps SBVTs for lightpath provisioning and hence each SBVT has 8 subcarriers, each of which can carry a 12.5Gbps signal in BPSK modulation format. A guard band with G = 2 spectrum slots is considered. Here, the increase in the traffic load is realized by increasing the numbers of VON requests coming into the networks.

In the online (dynamic) scenario, we carry out simulations to evaluate the performance of the proposed algorithms in a realistic Deutsche Telecom (DT) topology with 14 nodes and 23 links, over a Java-based simulation platform. The arrival of the VON requests follows the Poisson traffic model. The average duration time $\mu$ of each VON request is assumed to be a unit time 1, which means that the energy consumption of each VON request we calculate can also be regarded as its power consumption. Thus the value of the traffic load (i.e., $\lambda/\mu$) is also equal to that of the request arrival rate $\lambda$. The rest of the simulation parameters are showed in Table 1. Note that in the DT topology, the bandwidth capacity of each VOL is set to be 320.

*Benchmark Algorithm:* We serve the traffic-load balancing (TB) scheme in the literature [13] as a benchmark algorithm. It tries to map evenly the VNs to the SNs to maintain TB. The TB scheme is not energy-efficient, since it has no any energy-saving consideration. Its main idea is to improve the request blocking probability.

In our online simulations, we propose two VONE schemes. The first scheme just considers the DC energysaving in the node mapping, and it assumes that the NS-BVT is used in each SN without optical traffic grooming. We denote it as "DC energy aware" scheme (i.e., DC-EA scheme). Therefore, the DC-EA scheme has no attempt for TP energysaving in the link mapping. The second scheme simultaneously considers the energy saving for the both DCs in the node mapping and TPs in the link mapping. We name it as "DC and TP energy aware" scheme (i.e., DA&TP-EA scheme). In the comparison with the two other schemes, the advantages of the proposed DA&TP-EA scheme can be quantified in a realistic network scenario in order to demonstrate whether the TP power savings are significant.

The formulations of the average power consumption (PC) per accommodated VON request, including the TP-PC and DC-PC parts, have been given out in Eq. (5)-(8) of the section IV. We also evaluate the resource utilizations of the DCs, the TPs, and the fiber links for the proposed algorithms in the 14-node DT topology. The definitions are shown as follows.

Resource utilization of all DCs in the SON:

$$U_{DC} = \frac{\sum_{g^v \in V_{accom}} \sum_{n^v \in N^v} c(n^v) \cdot \Delta T(g^v)}{\sum_{n^s \in N^s} C(n^s) \cdot \psi(dc_{n^s})} \tag{27}$$

where the $\psi(dc_{n^s}) = 1$ represents the DC attached with the SN $n^s$ is turned on during the simulation period and $V_{accom}$ represents the set of accommodated VONs. $\Delta T(g^v)$ denotes the lifetime of the VON request $g^v$.

Resource utilization of all TPs in the SON:

$$U_{TP} = \frac{\sum_{g^v \in V_{accom}} \sum_{l^v \in L^v} tr(l^v) \cdot \Delta T(g^v)}{\sum_{alltp^k_{n^s}} TR^{\max}_{tp} \cdot \psi\left(tp^k_{n^s}\right)} \tag{28}$$

where the $\psi\left(tp^k_{n^s}\right) = 1$ represents the $k$-th sliceable-TP in the SN $n^s$ is turned on during the simulation period and the $TR^{\max}_{tp}$ is the maximum transmission rate of a sliceable-TP.

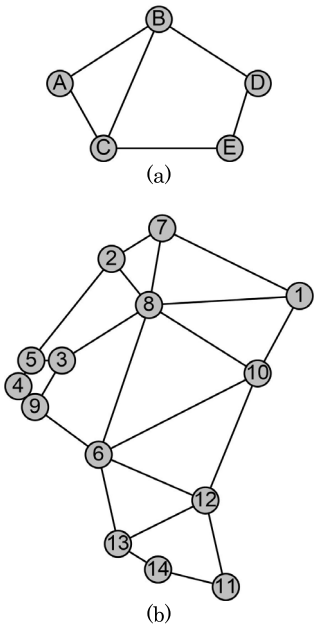


**FIGURE 4.** (a) Simple 5-node topology and (b) DT network.

Resource utilization of all links in the SON:

$$U_{Link} = \frac{\sum_{g^v \in V_{accom}} \sum_{l^v \in L^v} fs\,(g^v) \cdot \Delta T\,(g^v)}{\sum_{l^s \in L^s} FS^s \cdot \xi\,(l^s) \cdot T_{total}} \tag{29}$$

where $\xi\,(l^s) = 1$ represents a SFL $l^s \in L^s$ is used during the simulation period and $T_{total}$ is the total simulation time.

### B. COMPARISON OF OFFLINE ALGORITHM AND ILP MODEL

In the offline (static) scenario, Fig. 5 compares the results for heuristic offline algorithm and ILP model on the average PC per accommodated VON request, including the TP-PC and DC-PC parts. Overall, we can observe from Fig. 5(a) that a gradual decline in the PC per accommodated VON request for the both curves, as the number of VON request increases. It is because that there are more VON requests would share the idle PC of DCs and the overhead PC of TPs, which results in the decline of the average PC. The average TP-PC part per accommodated VON follows the same trend in Fig. 5(b), as the number of VON request increases. We also find from Fig. 5(a) that the ILP result is a bit better than that of the offline algorithm. It is mostly attributed to the difference of the average TP-PC between the offline algorithm and ILP model, while the average DC-PC difference is minimal, as shown in Fig. 5(b). Furthermore, the difference is mainly due to the incurred spectral fragments with the heuristic VONE algorithm, which leads to the increase of the number of used TPs in the VONE process and ultimately to the PC increase. Note that there is a hollow drop point in two curves in Fig. 5(a), when the number of VON requests is 4. The hollow drop point in Fig. 5(a) would be caused by

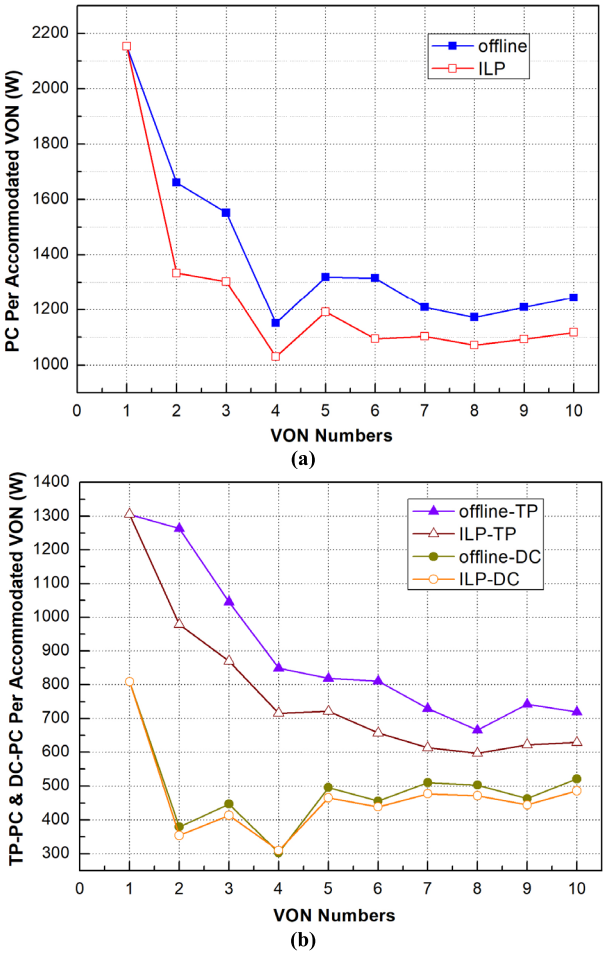


**FIGURE 5.** Comparison of heuristic offline algorithm and ILP model about (a) average power consumption (PC) per accommodated VON, including (b) average TP-PC.

the DC-PC per accommodated VON as shown in Fig. 5(b). It indicates that the provisioning process of the fourth VON request would not activate a new DC, and the VON can be accommodated well into the existing activated DCs. Hence, the DC-PC turns to a decline, compared to the DC-PC in case that the VON number is 3. From Fig. 5(b), we can conclude that the impact of the TP-PC is more important than that of the DC-PC part. Therefore, it is very necessary to consider the TP energy- saving for the energy-efficient VONE process.

### C. AVERAGE POWER CONSUMPTION

The simulation results in the online (dynamic) scenario are given in the following. Here, the traffic load is measured in term of Erlangs. Fig. 6(a) gives out the results on the average PC per accommodated VON request for above three schemes under different traffic loads. Fig. 6(b) shows the power-saving ratio for each accommodated VON, compared with the TB scheme. It can be found from the above figures that the DC&TP-EA scheme archives the minimum average PC per accommodated VON. Compared with the TB scheme, the

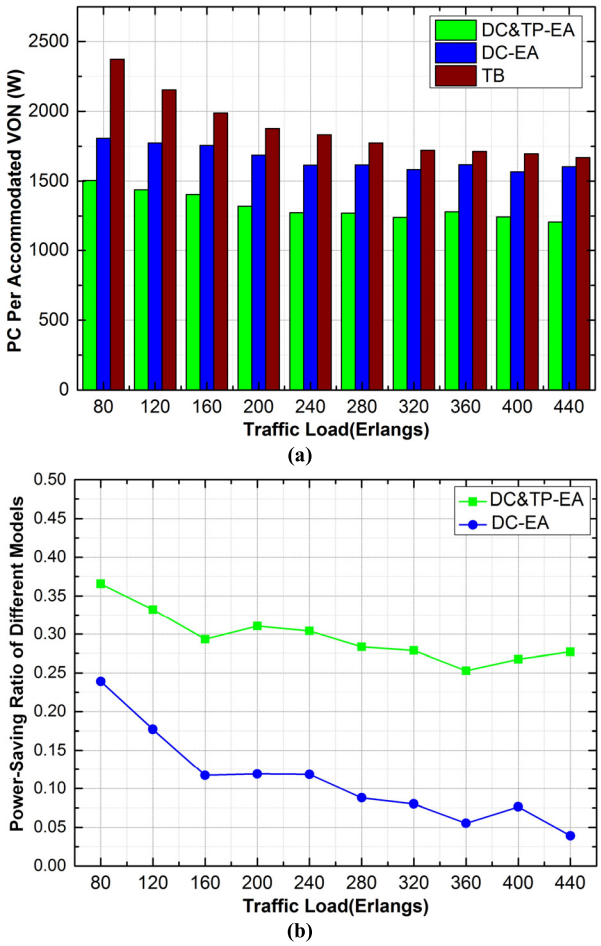


**FIGURE 6.** (a) Average PC per accommodated VON and (b) powersaving ratio per accommodated VON compared with the TB scheme.

DC&TP-EA can save up to 37% PC per accommodated VON request, and 30% in average. However, the DC-EA just can save maximum 24% PC compared with the TB scheme. It is due to the fact that the DC&TP-EA scheme simultaneously considers the energy saving of both the DCs and TPs, while the DC-EA scheme only considers the power saving for DCs. It is worthy to note that, in Fig. 6(a), with the increase of the traffic load, the PC gap between the TB scheme and other two schemes becomes smaller and smaller. And the power-saving ratio of the other two schemes is also decreasing as shown in Fig. 6(b). It is because that more and more DCs and TPs need to be activated for accommodating more VON requests. For the TB scheme, we find that the average PC per accommodated VON request decreases with the increase of the traffic load, since that in each SN, the idle/overhead power consumptions of the DCs/TPs are shared by more VON requests as the traffic load increases.

### D. AVERAGE TRAFFIC-DEPENDENT POWER CONSUMPTION

As stated in section III.D, those PC part independent of the traffic load (i.e., the idle PC of DCs and the overhead PC of TPs), would seriously deteriorate the VONE energy

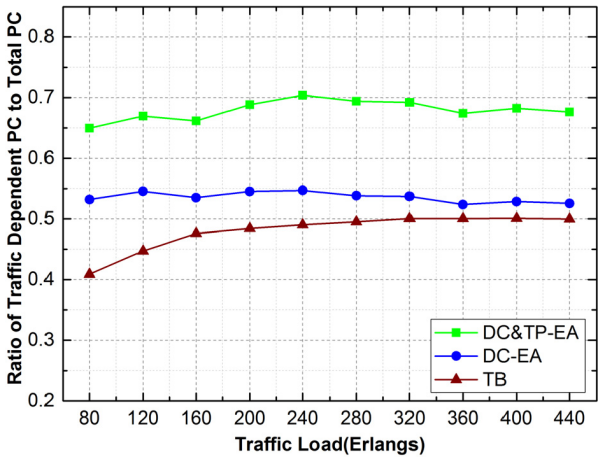


**FIGURE 7.** Ratio of traffic-dependent PC to total PC per accommodated VON.

saving performance. Hence, we can desire that the higher the ratio of the average traffic-dependent PC to total PC, the better the power efficiency. Fig. 7 shows the ratios of the average traffic-dependent PC to total PC for each accommodated VON under different traffic loads. We observe that the DC&TP-EA scheme has the highest ratio, followed by the DC-EA scheme, while the TB scheme presents the lowest ratio. The larger ratio value means that more power is served as the traffic-dependent power, which is consumed by VON requests rather than for waste. It is because that with the DC&TP-EA scheme, the resource utilization of both the DC and TP is higher (see more in Fig. 10). In other words, one DC or one TP can accommodate more VON requests in average. Note that the performance of the DC-EA scheme comes second, because that it just improves the utilization of the DCs by using the DC resource consolidation technique in the node mapping. It is also found that with the increase of traffic load, tow curves of the DC-EA and TB schemes gets closer. It indicates that when the traffic load is larger, the benefit from the DC-aware energy-saving technique is dwindling, while the effect of the TP-aware energy-saving becomes dominant. It confirms again that the significance of the TP energy-saving for the energy-efficient VONE process.

### E. AVERAGE IDLE/OVERHEAD POWER CONSUPTION

Fig. 8 shows idle/overhead power consumption of DCs and TPs per accommodated VON, respectively, which is main source of the energy waste. In Fig. 8(a), we can see that DC idle power consumptions of both the DC-EA and DC&TP-EA schemes are much smaller than that of the TB scheme. Moreover, as the traffic load increases, the idle power for the TB scheme becomes less and less, and gets closer to that of the two other schemes. It is because that the DC utilization of the TB scheme is continuously improved, as the traffic load increases (see Fig. 10(a)). We can observe from Fig. 8(b) that the DC&TP-EA scheme performs much better than two

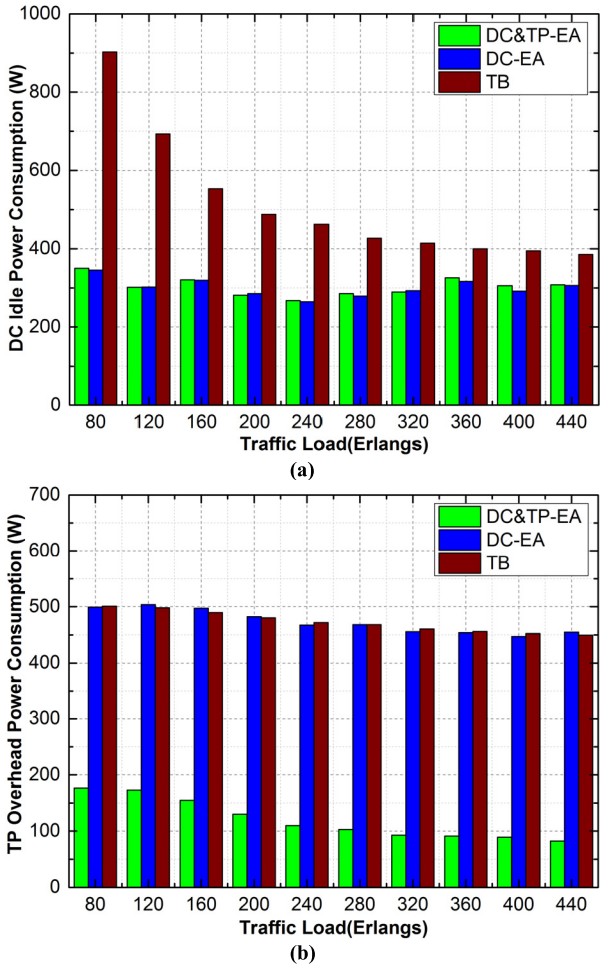


**FIGURE 8.** (a) DC idle power consumption and (b) TP overhead power consumption per accommodated VON.

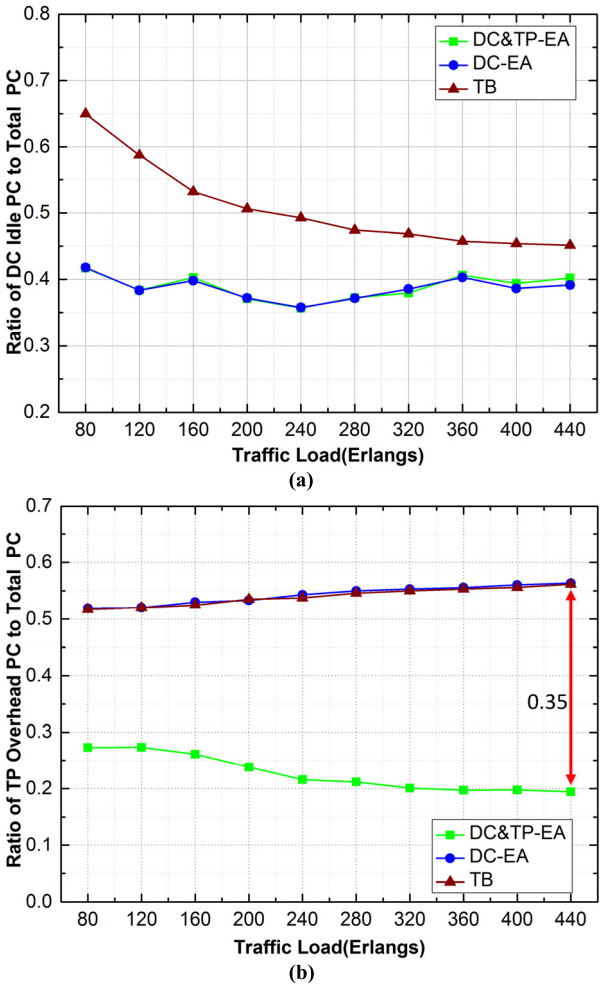


**FIGURE 9.** (a) Ratio of DC idle PC to total PC and (b) ratio of TP overhead PC to total PC per accommodated VON.

other schemes on the TP overhead PC. It is due to the fact that the DC&TP-EA scheme additionally considers the TP energy saving, except for the DC energy saving. Moreover, the DC&TP-EA scheme would consume less and less average TP overhead power with the increase of traffic load, because that more VOL requests can be optically groomed into one physical SBVT, which improves greatly the TP utilization (see Fig. 10(b)).

Fig. 9 shows the ratio of idle/overhead PC to total PC per accommodated VON for the DCs and TPs under the different traffic loads, respectively. In Fig. 9(a), we can see that the TB scheme wastes the most PC compared to other two schemes, without any power-saving consideration. And the DC&TP-EA and DC-EA schemes show similar performance about the DC idle PC. We also find that the TB curve experiences a downward trend with the increase of traffic load, and in the case of the larger traffic load, the TB curve gets closer to the other two curves. It is due to the fact that more resources can be used effectively.

In Fig. 9(b), we can observe that the DC&TP-EA scheme saves up to 35% overhead PC of TPs at the load of 440 Erlang, compared with the two other schemes. With the increase of traffic load, the ratio of the TP overhead PC in the DC&TP-EA scheme further lowers, while the curves of the DC-EA and TB schemes show an upward trend. The major reason is that the DC&TP-EA can optically groom the incoming VOL requests into existing lightpaths with the aid of SBVTs. On the contrary, the DC-EA and TB schemes have to active a new NS-BVT to establish a new lightpath for the incoming VOL request, which will inevitably reduce the TP utilization and produce more TP overhead PC.

According to Fig. 9, we can conclude that when the traffic load is larger, the impact of the TP energy-saving is much more important than that of the DC energy-saving, and thus the TP-aware energy-saving solution for the VONE becomes extremely necessary.

### F. RESOURCE UTILIZATION IN SONS

Fig. 10 shows the resource utilization of the DCs and TPs in the SON under the different traffic loads. In Fig. 10(a), we can see that the DC-EA and DA&TP-EA schemes achieve higher

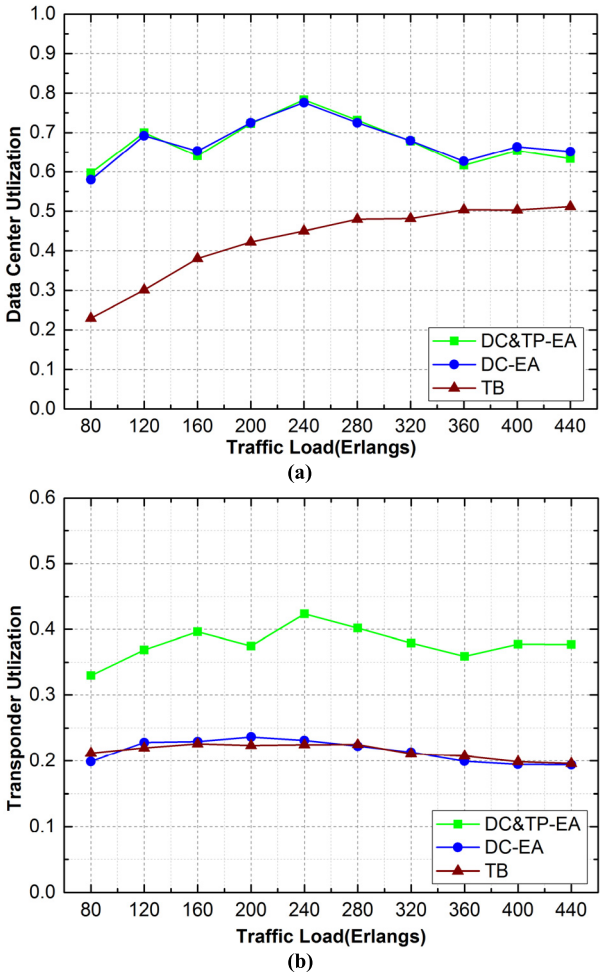


**FIGURE 10.** Resource utilization of (a) the DCs and (b) the TPs under different traffic loads.

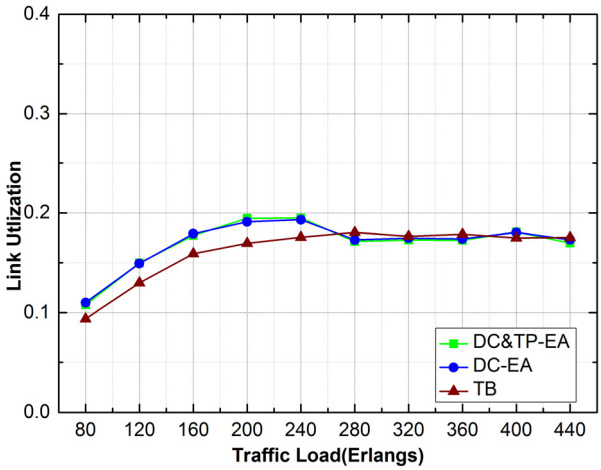


**FIGURE 11.** Link utilization in the SON.

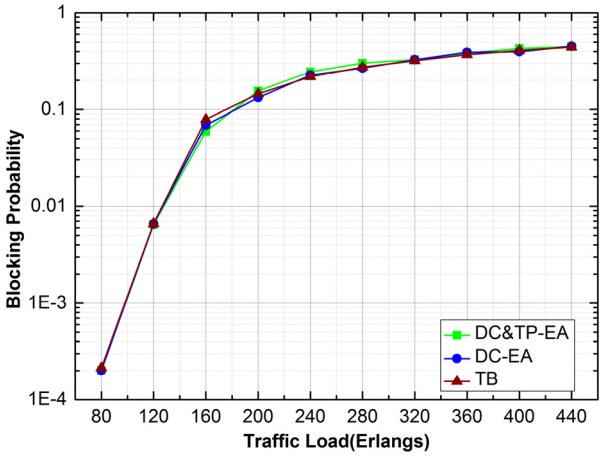


**FIGURE 12.** VON request blocking probability.

DC utilization than the TB scheme due to the fewer DCs activated, which is due to using resource consolidation of the DCs in the node mapping (see Algorithm 1). With the increase of traffic load, the DC utilization of the TB scheme shows a growing trend. It is because that more and more VON requests can be accommodated in the activated DCs. Note that the DC utilization of the DC-EA and DA&TP-EA fluctuations up and down in the range from 0.6 to 0.8. The up-trend line indicates that more VON requests can be accommodated just into the existing active DCs, while the down-trend line represents some new DCs are activated for new-coming VON requests. In Fig. 10(b), it is observed that the TP utilization of the DC&TP-EA scheme is much better than that of two other schemes. The main reason is that with the aid of the SBVT, the DC&TP-EA can optically groom more VOL requests into the one existing activated TP during link mapping procedure. But, for the DC-EA and TB schemes, the TP (i.e., NS-BVT) utilization is lower due to its single- flow operation. For instance, one VOL request that only requires 25Gbps traffic is running on the 100Gbps NS-BVT, which would cause serious resource waste of the TP.

Additionally, we can also investigate the link utilization of the SON in Fig. 11. When the traffic load is smaller, the link utilization of the DC&TP-EA and DC-EA schemes performs a slight better than the TB scheme. This is because that with the DC&TP-EA and DC-EA schemes, only a very few SNs can be activated to provision the VNs, and thus it is possible that the existing routes are re-used by more accommodated VON requests. Hence, the link utilization can be improved. However, with the increase of traffic load, more and more SNs should be activated, and thus more and more routes can be adopted. Therefore, the link utilizations of the three schemes present similar trend eventually.

### G. GVON REQUEST BLOCKING PROBABILITY

Fig. 12 shows the VON request blocking probabilities for the three schemes. We observe that our proposed two schemes have similar blocking probability performance as the TB scheme, in addition to the outstanding power-saving performance. The main idea behind this TB scheme is to improve the blocking probability. Therefore, the simulation results

demonstrate the effectiveness and superiority of our proposed schemes for the energy-efficient VONE.

## VII. CONCLUSIONS

We investigated the performances of the proposed energy efficient VONE schemes over transparent EONs equipped with SBVTs. To the best of our knowledge, we are the first to come up with the scheme that simultaneously considering the TP reusability and the DC consolidation for power- efficient VONE. More specifically, we introduce the DC node consolidation technique into the node mapping algorithm; meanwhile for the link mapping, we adopt the optical traffic grooming strategy to improve the capacity of the SBVTs, which is equipped within each SN. A novel energy- minimized traffic-grooming-enabled ILP model is proposed. For scalability, the static (offline) and dynamic (online) energy-efficient VONE algorithms are designed for large network instances. The simulation results show that the DC&TP-EA scheme can achieve up to 37% power saving compared with the TB scheme. Also, the effect of DC energy saving is very remarkable in the DC-EA or DC&TP-EA scheme when the traffic load is smaller. With the increase of traffic load, the DC energy saving may matter less, while the TP energy-saving plays a more and more important role. In addition, both the DC&TP-EA and DC-EA schemes have similar blocking performance as that of the TB scheme, which just aims to improve request blocking probability without any energy-saving consideration. These results demonstrate the effectiveness and superiority of our proposed schemes for the energy-efficient VONE.

## REFERENCES

[1] N. M. M. K. Chowdhury and R. Boutaba, "A survey of network virtualization," *Comput. Netw.*, vol. 54, no. 5, pp. 862–876, Apr. 2010.
[2] United States Environmental Protection Agency. (2007). *Report to Congress on Server and Data Center Energy Efficiency Public Law 109-431*. [Online]. Available: http://www.energystar.gov/ia/partners/prod_development/downloads/EPA_Datacenter_Report_Congress_Final1.pdf
[3] S. Figuerola and M. Lemay, "Infrastructure services for optical networks," *J. Opt. Commun. Netw.*, vol. 1, no. 2, pp. A247–A257, Jul. 2009.
[4] J. Zhang *et al.*, "Dynamic virtual network embedding over multilayer optical networks," *J. Opt. Commun. Netw.*, vol. 7, no. 9, pp. 918–927, Sep. 2015.
[5] J. Zhang *et al.*, "Dynamic traffic grooming in sliceable bandwidth-variable transponder-enabled elastic optical networks," *J. Lightw. Technol.*, vol. 33, no. 1, pp. 183–191, Jan. 1, 2015.
[6] J. Zhang *et al.*, "Energy-efficient traffic grooming in sliceable-transponder-equipped IP-over-elastic optical networks," *J. Opt. Commun. Netw.*, vol. 7, no. 1, A142-A152, Jan. 2015.
[7] M. Jinno, H. Takara, Y. Sone, K. Yonenaga, and A. Hirano, "Multiflow optical transponder for efficient multilayer optical networking," *IEEE Commun. Mag.*, vol. 50, no. 5, pp. 56–65, May 2012.
[8] M. Zhu, P. Gao, J. Zhang, X. Zeng, and S. Zhang, "Energy efficient dynamic virtual optical network embedding in sliceable-transponder-equipped EONs," in *Proc. IEEE Global Commun. Conf.*, Singapore, Dec. 2017, pp. 1–6.
[9] J. F. Botero, X. Hesselbach, M. Duelli, D. Schlosser, A. Fischer, and H. de Meer, "Energy efficient virtual network embedding," *IEEE Commun. Lett.*, vol. 16, no. 5, pp. 756–759, May 2012.
[10] S. Su, Z. Zhang, X. Cheng, Y. Wang, Y. Luo, and J. Wang, "Energy-aware virtual network embedding through consolidation," in *Proc. IEEE INFOCOM Workshops*, Orlando, FL, USA, Mar. 2012, pp. 127–132.
[11] S. Su, Z. Zhang, A. X. Liu, X. Cheng, Y. Wang, and X. Zhao, "Energy-aware virtual network embedding," *IEEE/ACM Trans. Netw.*, vol. 22, no. 5, pp. 1607–1620, Oct. 2014.
[12] A. Pagès, J. Perelló, S. Spadaro, J. A. García-Espín, J. F. Riera, and S. Figuerola, "Optimal allocation of virtual optical networks for the future Internet," in *Proc. 16th Int. Conf. Opt. Netw. Design Modeling*, Colchester, U.K., Apr. 2012, pp. 1–6.
[13] L. Gong and Z. Zhu, "Virtual optical network embedding (VONE) over elastic optical networks," *J. Lightw. Technol.*, vol. 32, no. 3, pp. 450–460, Feb. 1, 2014.
[14] S. Zhang and B. Mukherjee, "Energy-efficient dynamic provisioning for spectrum elastic optical networks," in *Proc. IEEE Int. Conf. Commun.*, Ottawa, ON, Canada, Jun. 2012, pp. 3031–3035.
[15] J. Zhang, Y. Zhao, J. Zhang, and B. Mukherjee, "Energy efficiency of IP-over-elastic optical networks with sliceable optical transponder," in *Proc. OFC*, San Francisco, CA, USA, Mar. 2014, pp. 1–3.
[16] L. Nonde, T. E. H. El-Gorashi, and J. M. H. Elmirghani, "Energy efficient virtual network embedding for cloud networks," *J. Lightw. Technol.*, vol. 33, no. 9, pp. 1828–1849, May 1, 2015.
[17] S. Zhang, L. Shi, C. S. K. Vadrevu, and B. Mukherjee, "Network virtualization over WDM networks," in *Proc. 5th IEEE Int. Conf. Adv. Telecommun. Syst. Netw.*, Bangalore, India, Dec. 2011, pp. 1–3.
[18] M. Yu, Y. Yi, J. Rexford, and M. Chiang, "Rethinking virtual network embedding: Substrate support for path splitting and migration," *ACM SIGCOMM Comput. Commun. Rev.*, vol. 38, no. 2, pp. 17–29, Apr. 2008.
[19] R. Nejabati, E. Escalona, S. Peng, and D. Simeonidou, "Optical network virtualization," in *Proc. 15th Int. Conf. Opt. Netw. Design Modeling*, Bologna, Italy, Feb. 2011, pp. 1–5.
[20] S. Azodolmolky *et al.*, "Experimental demonstration of an impairment aware network planning and operation tool for transparent/translucent optical networks," *J. Lightw. Technol.*, vol. 29, no. 4, pp. 439–448, Feb. 15, 2011.
[21] Principled Technologies. (2012). *Advanced Power Management With Dell Open Manage Power Center*. [Online]. Available: http://www.principledtechnologies.com/Dell/R720_power_0312.pdf

Authors' photographs and biographies not available at the time of publication.